Article

Cell Reports

# Single-Cell Lineage Tracing Reveals that Oriented Cell Division Contributes to Trabecular Morphogenesis and Regional Specification

## Graphical Abstract

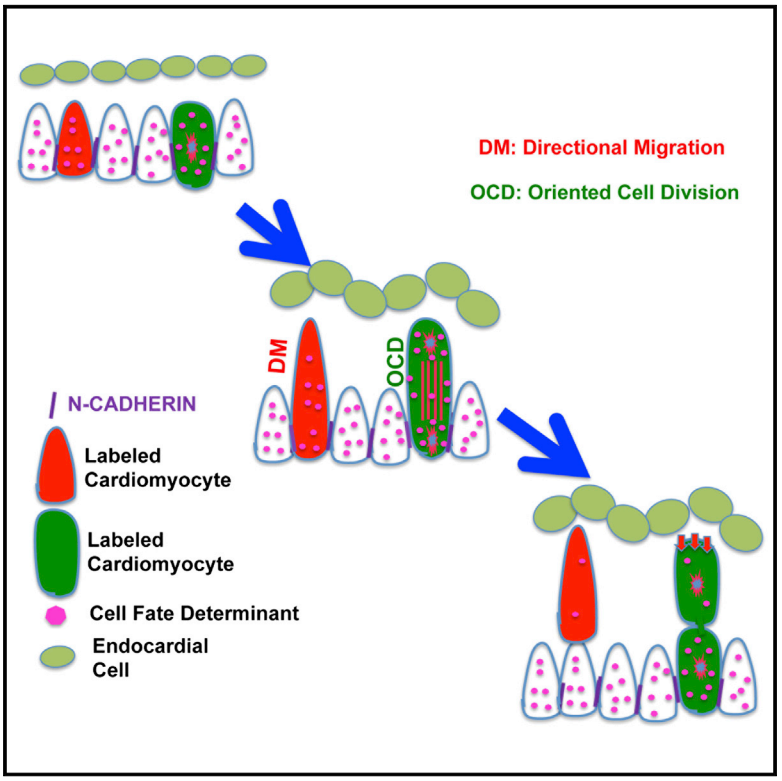


## Authors

Jingjing Li, Lianjie Miao, David Shieh, ..., Harold A. Singer, Guoying Huang, Mingfu Wu

## Correspondence

wum@mail.amc.edu

## In Brief

Li et al. used single-cell lineage tracing to demonstrate that both OCD and directional migration contribute to cardiac trabecular initiation. N-Cadherin regulates trabeculation via controlling OCD and directional migration in a cell-autonomous manner. Perpendicular OCD is an extrinsic asymmetric cell division and contributes to trabecular regional specification.

## Highlights

- Establish single-cell lineage tracing and whole-heart clearing and imaging
- Oriented cell division (OCD) and directional migration contribute to trabeculation
- OCD is an extrinsic asymmetric cell division
- OCD contributes to trabecular regional specification

Li et al., 2016, Cell Reports *15*, 158–170
April 5, 2016 
http://dx.doi.org/10.1016/j.celrep.2016.03.012

OPEN ACCESS
CellPress

Cell Reports
Article

# Single-Cell Lineage Tracing Reveals that Oriented Cell Division Contributes to Trabecular Morphogenesis and Regional Specification

Jingjing Li,[1] Lianjie Miao,[1] David Shieh,[1] Ernest Spiotto,[1] Jian Li,[2] Bin Zhou,[3] Antoni Paul,[1] Robert J. Schwartz,[4] Anthony B. Firulli,[5] Harold A. Singer,[1] Guoying Huang,[2] and Mingfu Wu[1,*]
[1]Center for Cardiovascular Sciences, Albany Medical College, Albany, NY 12208, USA
[2]Key Laboratory of Molecular Medicine, Ministry of Education, Fudan University, Shanghai 200032, China
[3]Department of Genetics, Albert Einstein College of Medicine, Yeshiva University, Bronx, NY 10461, USA
[4]Biology and Biochemistry, University of Houston, Houston, TX 77204-5001, USA
[5]Riley Heart Research Center, Indiana University, Indianapolis, IN 46202, USA
*Correspondence: wum@mail.amc.edu
http://dx.doi.org/10.1016/j.celrep.2016.03.012

## SUMMARY

**The cardiac trabeculae are sheet-like structures extending from the myocardium that function to increase surface area. A lack of trabeculation causes embryonic lethality due to compromised cardiac function. To understand the cellular and molecular mechanisms of trabecular formation, we genetically labeled individual cardiomyocytes prior to trabeculation via the brainbow multicolor system and traced and analyzed the labeled cells during trabeculation by whole-embryo clearing and imaging. The clones derived from labeled single cells displayed four different geometric patterns that are derived from different patterns of oriented cell division (OCD) and migration. Of the four types of clones, the inner, transmural, and mixed clones contributed to trabecular cardiomyocytes. Further studies showed that perpendicular OCD is an extrinsic asymmetric cell division that putatively contributes to trabecular regional specification. Furthermore, N-Cadherin deletion in labeled clones disrupted the clonal patterns. In summary, our data demonstrate that OCD contributes to trabecular morphogenesis and specification.**

## INTRODUCTION

Trabeculae are sheet-like structures that extend from the myocardium into the heart lumen to increase surface area, facilitating nutrient and gas exchange (Sedmera and Thomas, 1996). In mouse embryo, cardiac trabeculation is initiated at embryonic day 9 (E9.0), and by E10.5 long and thin trabeculae are formed. Subsequently, the trabeculae largely coalesce into the ventricular wall to thicken the compact myocardium. A lack of trabeculation causes embryonic lethality, whereas trabeculae failing to undergo compaction will result in left ventricular non-compaction (LVNC) cardiomyopathy (Breckenridge et al., 2007; Gassmann et al., 1995; Jenni et al., 1999; Pignatelli et al., 2003; Towbin et al., 2015; Weiford et al., 2004; Zhao et al., 2014). Approximately half a million Americans suffer from compromised heart function due to LVNC (Finsterer, 2010). Despite the fundamental functions of trabeculation, the molecular and cellular mechanisms underlying this process are not fully understood.

The cellular and molecular mechanisms of mammalian cardiac morphogenesis as a whole remain unclear, partly due to the multiple cell types involved, the intricate signaling interactions, and the challenges of analyzing the dynamic cellular behaviors during heart morphogenesis. Previously, sparse cell labeling via autonomous intragenic recombination has shown that myocardial precursors undergo the following two different phases of growth: dispersive growth along the venous-arterial axis of the cardiac tube and oriented coherent cell growth, characterized by a lower level of intermingling (Meilhac et al., 2003, 2004). Virally labeled cells of the pre-cardiac mesoderm proliferate and form wedge-shaped colonies, with wider outer sides and narrower inner (luminal) sides (Meilhac et al., 2003; Mikawa et al., 1992a, 1992b). However, interpretations of these data are limited by the uncontrolled timing of single-cell labeling, and imaging the labeled cells has been limited to the heart surface or two-dimensional analysis. To obtain a more comprehensive understanding of the mechanisms of trabecular morphogenesis, three-dimensional (3D) level imaging is required. Recently developed approaches including mosaic analysis with double markers and inducible multicolor labeling systems such as the brainbow system (Livet et al., 2007) have been used to determine early mesoderm progenitor specification (Chabab et al., 2016; Devine et al., 2014; Gupta and Poss, 2012; Lescroart et al., 2014). Applying such controllable inducible systems combined with 3D imaging to determine the cellular and molecular mechanisms underlying heart morphogenesis, especially trabeculation, has not yet been reported.

Previous work has shown that trabecular and compact cardiomyocytes display different features. Trabecular cardiomyocytes exhibit a lower proliferation rate and molecularly are

more mature than cardiomyocytes of the compact zone (Sedmera et al., 2003). Differential expression patterns are well established between the trabecular and compact zones. For example, *p57*, *Irx3*, *BMP10*, and *Cx40* are highly expressed in the trabecular zone, whereas *Tbx20*, *Hey2*, and *N-Myc* are highly expressed in the compact zone (Chen et al., 2004; Kochilas et al., 1999; Sedmera et al., 2000; Zhang et al., 2013). However, the mechanisms underlying the different cardiomyocyte specification between the two zones are unknown.

In order to investigate trabecular morphogenesis and regional specification in mice, we employed the inducible multicolor brainbow system and the embryo clearing system to genetically label, trace, image, and analyze cardiomyocytes at the single-cell level (Hama et al., 2011; Livet et al., 2007; Susaki et al., 2014). The improved imaging depth and scale of the cleared embryos allow for comprehensive 3D imaging and reconstruction of the heart and analysis of a single cell with spatial detail at the whole-heart scale. This enables us to determine the cellular dynamics and differentiation of cardiac progenitors in vivo during trabeculation. In contrast to zebrafish, in which trabeculation is initiated only by directional migration of cardiomyocytes from the compact zone (Gupta and Poss, 2012; Liu et al., 2010; Peshkovsky et al., 2011; Staudt et al., 2014), we found that in a mammalian system labeled cardiomyocytes undergo either oriented cell division (OCD) or directional migration toward the cardiac lumen, resulting in trabecular formation and regional specification. To further confirm that OCD is required for trabeculation, we disrupted the adherens junctions which are required to establish OCD (den Elzen et al., 2009) by deleting *Cdh2*, the gene encoding N-Cadherin (N-CAD), in the whole heart or in a single labeled cardiomyocyte. Cardiac-specific *Cdh2* knockout (CKO) displayed trabeculation defects, and *Cdh2* null clones in a mosaic heart were localized to the heart surface, indicating that both N-CAD-dependent OCD and directional migration are required for trabeculation.

To determine whether OCD is an asymmetric cell division that contributes to differential specification between the compact and trabecular zones, we examined the distribution of mRNAs in the dividing cells and the resulting two daughter cells. We found that the mRNAs are not asymmetrically distributed within the dividing cells, but after division, the two daughter cells of a perpendicular OCD display distinct levels of mRNAs. This suggests that the different geometric locations or the different signals that the two daughter cells receive cause the asymmetric levels of mRNAs. This phenomenon is known as an extrinsic asymmetric cell division and has been well-documented previously in *Drosophila* ovarian stem cells (Knoblich, 2008). We further studied the function of N-CAD in trabecular regional specification and found that, whereas the *Cdh2 CKO* displayed specification defects, the *Cdh2* null clones in a mosaic mouse model did not, indicating that N-CAD does not regulate cell-autonomous cardiomyocyte specification.

## RESULTS

### Imaging a Labeled Cell inside the Cleared Heart

Single-cell tracing and analysis at the whole-heart scale during cardiac development is essential to determine the cellular dynamics and differentiation of cardiac progenitor cells in vivo, but is hindered by the lack of imaging depth due to tissue opacity and light scattering. To overcome these obstacles, we adapted the following system that can render the heart highly transparent for both illumination and detection: whole-embryo clearing (Figure 1A; Figures S1A and S1B) (Hama et al., 2011; Susaki et al., 2014; Wu et al., 2010; Zhao et al., 2014). To distinguish endocardial cells from cardiomyocytes, embryos were stained for the endothelial cell marker PECAM in the far-red channel and counter-stained with DAPI in the blue channel to identify the geometric location of each cell in the heart. Individual cardiomyocytes inside the cleared heart are visible and can be imaged via confocal microscopy (Figure 1B). Cell orientation, division patterns, and geometric localization of the labeled cells in the heart can be determined with Imaris software (Figure 1B; Movie S1). To generate single-cell clones in a temporally controlled manner, we crossed *iCre* (Badea et al., 2003), whose Cre nuclear localization can be induced by tamoxifen, with the reporter mouse *Conf* (Livet et al., 2007). *Conf* reporter mice in theory can stochastically generate nuclear green, cytoplasmic yellow, cytoplasmic red, or membrane-bound CFP upon transient Cre-mediated recombination in an individual cell (Figures S1C and S1D) (Livet et al., 2007). To determine the timing of labeling, we gavaged pregnant females bearing E7.75 embryos with tamoxifen at a dosage of 20 μg per gram of body weight (20 μg/g). Although we did not observe any fluorescent cells 12 hr after induction, after 16 hr individual fluorescent cells were observed in the *iCre;Conf* hearts (Figure 1C). At a dosage of 20 μg/g, the number of recombinant fluorescent clones in the ventricle 24 hr after induction is not significantly different from the number of clones 72 hr after induction (Figure 1D), indicating that a single dose of tamoxifen at a concentration of 20 μg/g or lower does not cause continuous labeling in the heart. To determine the dosage of tamoxifen required to label a single cell of an embryonic heart tube at around E8.0–E8.5, we induced transient Cre activation using different dosages of tamoxifen when the embryos were at E7.75. We quantified the number of recombined clones (recombined blue clones were not quantified due to DAPI staining) per ventricle 72 hr after induction and found that the number of clones in the ventricle was tamoxifen dosage dependent (Figure 1E). Tamoxifen at 10 μg/g induced one or no recombination event in the primitive ventricle (Figure 1E) and was used for the following lineage tracing experiments unless otherwise specified. It is interesting to note that this concentration is higher than the previously reported 4 μg/g that can induce single recombination in the embryonic retina, and the difference might be due to different reporter mouse lines used and different organs examined (Badea et al., 2003). Probabilistic calculations indicated that a dosage of 10 μg/g can be used to induce clonal analysis with a very low risk of adjacent cell labeling, as detailed in the Supplemental Information and Figures S2A and S2B.

### Cardiomyocyte Clones Display Four Types of Geometric Patterns

To determine cellular dynamics during trabecular initiation, pregnant females were gavaged with tamoxifen when the

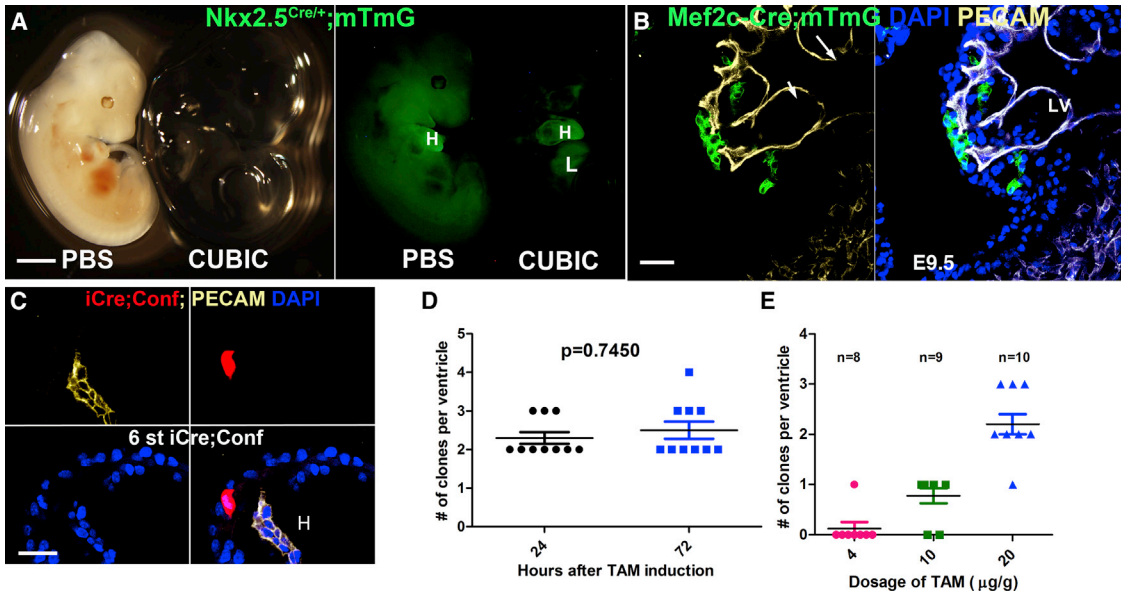


**Figure 1. Whole-Embryo Clearing to Image a Single Clone inside a Heart**

(A) *Nkx2.5*$^{Cre/+}$*;mTmG* embryos at E12.5 were cleared in CUBIC reagents or in PBS as a control. H, heart; L, liver.

(B) Single GFP cells inside the SCALE-treated *Mef2c-Cre;mTmG* heart at E9.5 can be imaged. LV, left ventricle.

(C) Single *iCre;Conf* control clone of a 6 st (somite) embryo is shown.

(D) The number of clones per ventricle 24 hr after induction is not significantly different from that 72 hr after induction.

(E) The number of clones is tamoxifen dosage dependent.

Scale bars, 200 μm (A) and 20 μm (B and C).

embryos were at about E7.75, so that cardiomyocytes would be labeled at E8.0–E8.5, a stage when the myocardium consists of a single cell layer and the trabeculae are not yet initiated (Figures S3A and S3B). We obtained 286 E10.5 embryos that each contained a single clone in the ventricle. Of them, 67 were endothelial clones (Figures 2A and 2C) marked by PECAM staining (Movie S2), whereas 217 were cardiomyocyte clones (Figures 2A and 2D–2G; Movie S3). Because cardiomyocytes and endocardial cells are already segregated at E8.0–E8.5, we only observed two bi-potent clones that contained mostly cardiomyocytes and a few endothelial cells (data not shown).

72 hr after induction, the labeled single cell had undergone several rounds of cell divisions, and the clones exhibited specific geometric patterns. To better define the geometric patterns, we divided the myocardium into the following three zones: outer compact, inner compact, and trabecular (Figure 2B). Based on the geometric distribution and anatomical annotation of each clone, the clones were categorized into four different patterns. In one clonal pattern, cells are localized to outer compact, inner compact, and trabecular zones, with one cell of the clone remaining in the outer compact zone (Figure 2D; Movie S3). This type of clone was defined as a transmural clone. The second type, in which all the cells are in the outer compact layer of the myocardium, was defined as a surface clone (Figure 2E; Movie S4). The third type displays two or more cells in the outer compact zone and some cells in the inner compact zone or trabecular zone and was defined as a mixed clone (Figure 2F; Movie S5). In the fourth type, all the cells are in the inner compact zone and/or trabecular zone, and were defined as an inner clone (Figure 2G; Movie S6). Of the 217 cardiomyocyte clones, 73 (33%) were transmural clones, 62 (29%) were inner clones, 32 (15%) were surface clones, and 50 (23%) were mixed clones (Figure 2H).

## Inner, Transmural, and Mixed Clones Contribute to Trabeculation

We further characterized the clones by quantifying the location, size, and number of cells of each control and *Cdh2* null clone (the *Cdh* null clones will be explained later). Of the four types of clones, surface clones displayed the shortest depth (z), defined by the length from the heart surface to the cell that is furthest to the surface, whereas the inner clones invaded the deepest (Figure 3A). The length and width of the clones (from a surface view) were quantified as x and y to reflect lateral spread, and mixed clones had the largest lateral spread (Figures 3B and 3C). We also quantified cell numbers in the different clones and found that surface clones had the lowest, whereas mixed clones had the highest numbers of cells among the four types (Figure 3D). Based on the depth and length of x and y in Figures 3A–3C, we drew a schematic model of the four types of clones regarding their contribution to trabeculation (Figure 3E). The surface clone is localized at the outer compact zone, whereas the inner clone migrates furthest, with the majority of the inner clones localized inside the inner compact zone or trabecular zone. The transmural clone spans from the outer compact, to the inner compact, and to the trabecular zone, whereas the cells of the mixed clone usually reside in the outer

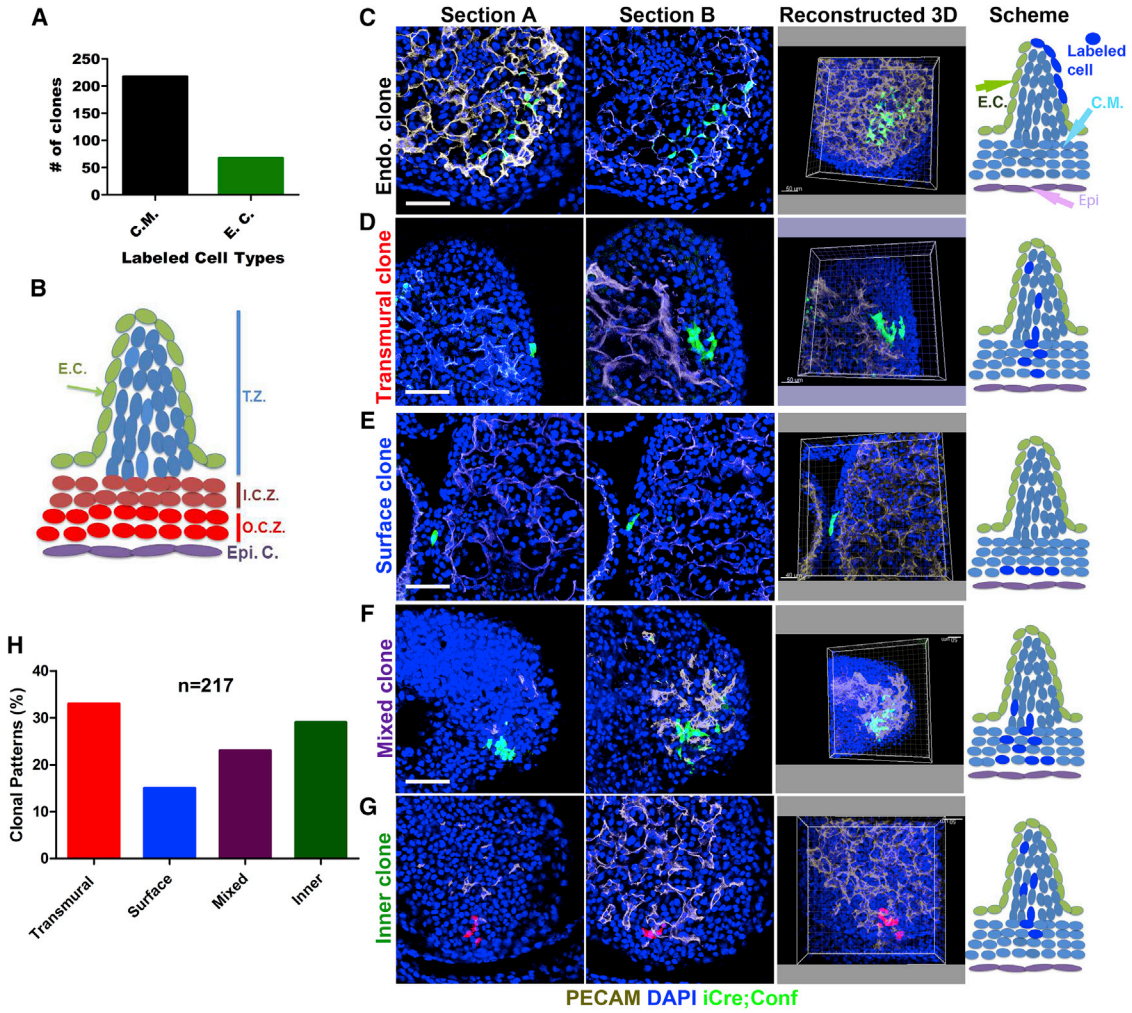


**Figure 2. Labeled Clones Display Four Types of Geometric Patterns**

(A) The number of clones of each cardiac cell type was identified.

(B) The different zones of the heart were schematically defined, including O.C.Z. (outer compact zone), I.C.Z. (inner compact zone), and T.Z. (trabecular zone).

(C–G) Sections A and B are two representative sections from a z stack of the same clone. The z stack was reconstructed to a 3D image. The scheme is an illustration to show the geometric pattern of the clone. (C) An endocardial cell clone. (D) A transmural clone. (E) A surface clone. (F) A mixed clone. (G) An inner clone.

(H) Percentage distribution of different types of clones is shown. E.C., endocardial cells; C.M., cardiomyocytes; Epi, epicardial cells.

Scale bars, 50 μm (C–G).

and inner compact zone with some cells are in the trabecular zone (Figures 3A and 3E).

## Myocardial Cell OCD Contributes to Different Clonal Patterns

We hypothesized that the clonal patterns are determined by the mitotic spindle orientation of the initial labeled cell. To determine mitotic spindle orientation of dividing cardiomyocytes during trabecular initiation, E9.0–E9.5 *Nkx2.5*$^{Cre/+}$*;mTmG* embryos were whole-mount stained with antibodies against acetylated α-tubulin and PECAM. We found that the majority of mitotic cells displayed either parallel orientation (40%, n = 75) with a spindle angle less than 30 degrees or perpendicular orientation (52%, n = 75) with an angle greater than 60 degrees relative to the heart surface (Figures 4A and 4B) (the division patterns of cardiomyocytes in *Cdh2 CKO* will be explained later).

To evaluate the OCD of cardiomyocytes in vivo, we examined labeled cardiomyocytes 24 hr after tamoxifen administration using the *iCre;Conf* system and found that within that time frame most labeled cells undergo one round of division to yield two cells (Figures 4C–4E). Since one daughter cell is at the surface of the compact zone, and the other daughter is in the trabecular zone or inner compact zone (Figure 4C), we infer that the two daughter cells resulted from a perpendicular division. When both daughter cells are in the compact zone, it suggests a parallel division (Figure 4D). In a migratory clone, the labeled cells migrate away from the outer compact zone

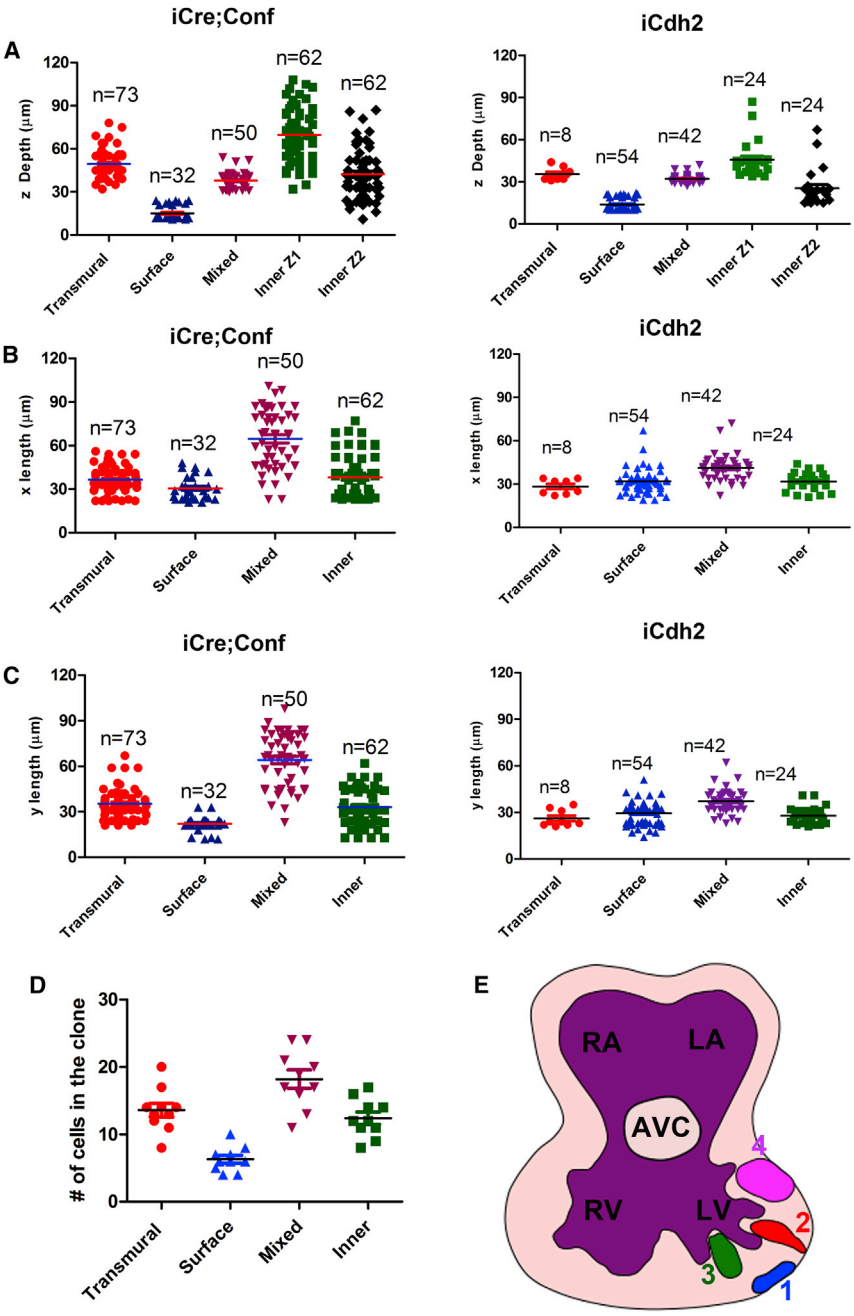


**Figure 3. Inner and Transmural Clones Contribute to Trabeculation**

(A–C) Comparison of the values of x (B), y (C), and z (A) in different types of clones between control and *iCdh2* null clones. z is the depth from the heart surface to the cell that is the furthest away from the heart surface, and x and y are the lengths the clone spans in the x and y axis, respectively. For the inner clone, z1 and z2 are respectively the distances of the furthest cell and the closest cells to the heart surface.

(D) Shows the number of cells in four different types of control clones. 10 clones from each type were presented.

(E) The distribution of the four control clones: 1, surface clone; 2, transmural clone; 3, inner clone; and 4, mixed clone in the heart. RV, right ventricle; LV, left ventricle; RA, right atrium; LA, left atrium; AVC, atria-ventricular cushion.

into the heart (Figure 4E) (Staudt et al., 2014). To determine whether the cardiomyocytes can further undergo OCD at later stages, we labeled the cells by gavaging tamoxifen to pregnant females when the embryos were at E8.75, at a concentration of 20 μg/g for 24 hr (considering that the E8.75 heart contains more cells and clones labeled for 24 hr contain only 1–3 cells, the probability of adjacent labeling with a tamoxifen concentration at 20 μg/g remains low). We found that the percentages of cells labeled at E7.75 and E8.75 that undergo perpendicular division were 43% (n = 57) and 40% (n = 66), respectively, which is not significantly different.

## OCD and Directional Migration Contribute to Trabeculation in an N-CAD-Dependent Manner

Previous work has shown that N-CAD, a component of adherens junctions, is essential for trabeculation (Ong et al., 1998). The *Cdh2 CKO* embryos die before E10.5 as previously reported (Luo et al., 2001). A BrdU pulse-labeling assay revealed that *Cdh2* null cardiomyocytes displayed a significantly lower proliferation rate compared to control (data not shown). *Cdh2* deletion causes cardiomyocytes to be loosely associated (Luo et al., 2001), and some hearts exhibited an absence of trabeculae and an abnormal morphology (Figures 5A and 5B), whereas others contained loose cardiomyocytes within the heart lumen (data not shown). The mitotic spindle orientation pattern of the CKO cardiomyocytes is significantly different from that of the controls (Figures 4A and 4B) (chi = 94.898, degrees of freedom [df] = 2, $p < 0.0001$), with parallel divisions occurring at a frequency of 37% and perpendicular at 29% (n = 35) (Figures 4A and 4B). However, the random mitotic orientation of CKO cardiomyocytes might be due to cardiac growth arrest, and whether it contributes to the trabeculation defects is not clear. To avoid cardiac growth arrest and further study how N-CAD regulates trabeculation, we labeled and deleted *Cdh2* within individual cells of *iCre;Conf*;*Cdh2*$^{fl/fl}$ (*iCdh2*) hearts by inducing Cre activation at E7.75 and examined the clonal patterns and distributions of *iCdh2* clones 72 hr later. The deletion of *Cdh2* within the *iCdh2* null clone was confirmed by N-CAD staining, and 78% (n = 23) of the labeled clones displayed absence of N-CAD (Figure 5C). We observed that 42% of the *iCdh2* clones are surface clones, 6% are transmural

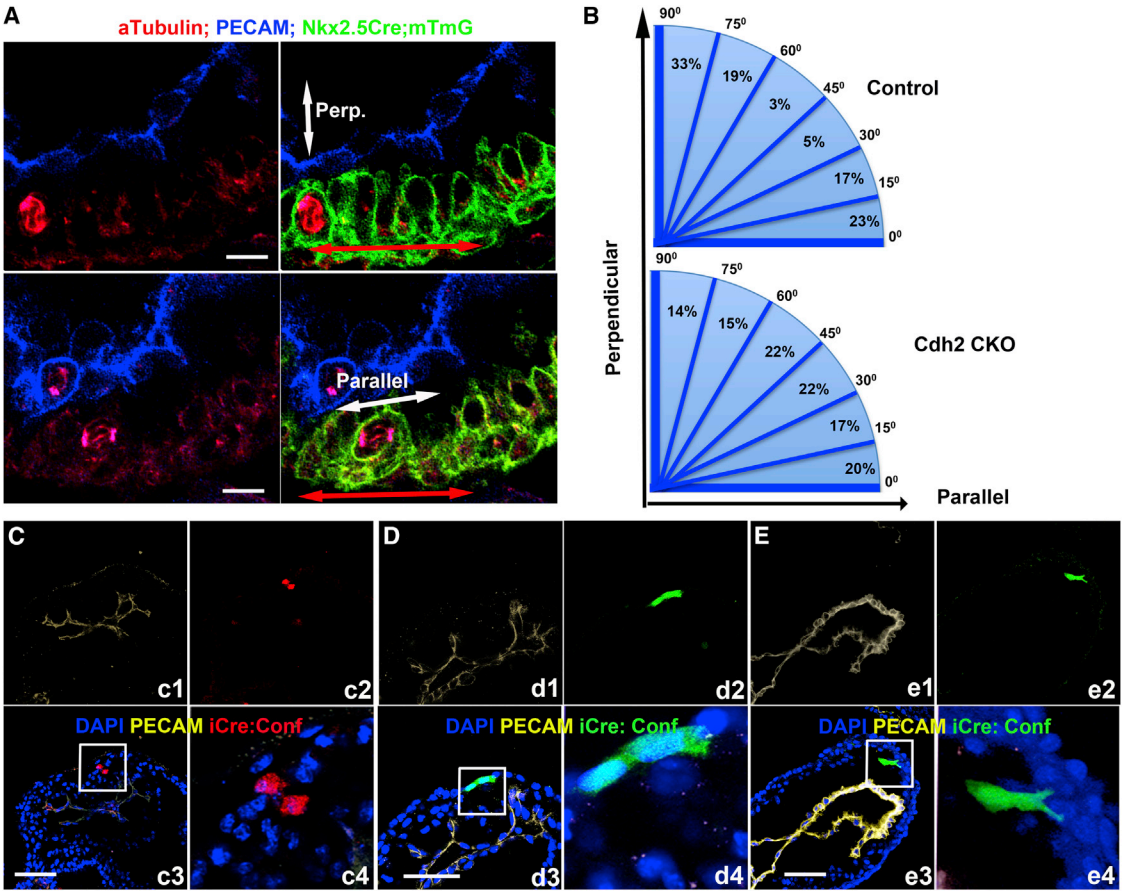


**Figure 4. Myocardial Cells Undergo Parallel and Perpendicular Divisions**

(A) E9.0–9.5 hearts were whole-mount stained with acetylated α-tubulin and PECAM. Images show that cardiomyocytes undergo perpendicular (perp.) and parallel divisions.

(B) The mitotic spindle orientation patterns of cardiomyocytes from control and *Cdh2 CKO* at E9.0–E9.5 hearts. The horizontal line represents the axis of heart surface, and the blue line represents an angle between mitotic spindle and heart surface. The number between blue lines indicates the percentage of cells whose mitotic spindle angle is between the two angles represented by the blue lines.

(C–E) *iCre;Conf* embryos were induced with tamoxifen at E7.75 and were examined 24 hr after induction. The labeled cells could undergo perpendicular division (C), parallel division (D), and directional migration (E). There are four quadrants in (C)–(E). c1, d1, and e1 are the PECAM staining; c2, d2, and e2 show the fluorescent protein; c3, d3, and e3 show the merged pictures; and c4, d4, and e4 show the enlarged quadrant in c3, d3, and e3, respectively.

Scale bars, 10 μm (A) and 50 μm (C–E).

clones, 19% are inner clones, and 33% are mixed clones (n = 128) (Figure 5D). These observations are significantly different from the clonal patterns in the controls (Figure 5D; chi = 147.151, df = 3, $p < 0.0001$). In addition, the overall geometric location of *iCdh2* clones is different from that of the control clones, as the *iCdh2* clones primarily localized to the heart surface and failed to invade deeply into the heart when compared to control clones (Figures 5E and 3A–3C; Movie S7). Furthermore, unlike the cells in the control clone, which are dispersed (Figures 2D, 2F, and 2G), many cells in the *iCdh2* clones are physically connected, suggesting invasion and migration defects (Figure 5E). The reduced number of transmural, inner, and mixed clones and the reduced invasion of all the clones might contribute to the trabeculation defects of the *Cdh2 CKO* hearts and indicates that N-CAD regulates trabeculation in a cardiomyocyte-autonomous manner. We quantified the number of cells per clone and found that the clone size of *iCdh2* is significantly smaller than that of the control clones (Figure 5F).

## OCD Contributes to Trabecular Regional Specification via a Mechanism of Extrinsic Asymmetric Cell Division

Trabecular cardiomyocytes are more differentiated than compact cardiomyocytes, although the molecular features and underlying mechanisms of the difference are unknown (Kochilas et al., 1999; Sedmera et al., 2000; Zhang et al., 2013). To determine their distinct specification at an early stage, we adapted an RNAscope ISH/IFS system, in which single mRNAs and certain proteins can be detected simultaneously. We screened several mRNAs including *Bmp10* (Chen et al., 2004), *Hey2* (Koibuchi and Chin, 2007), and *Irx3* (Christoffels et al., 2000), which were previously reported to be differentially expressed in compact and trabecular zones at certain stages, and Ppib, which encodes

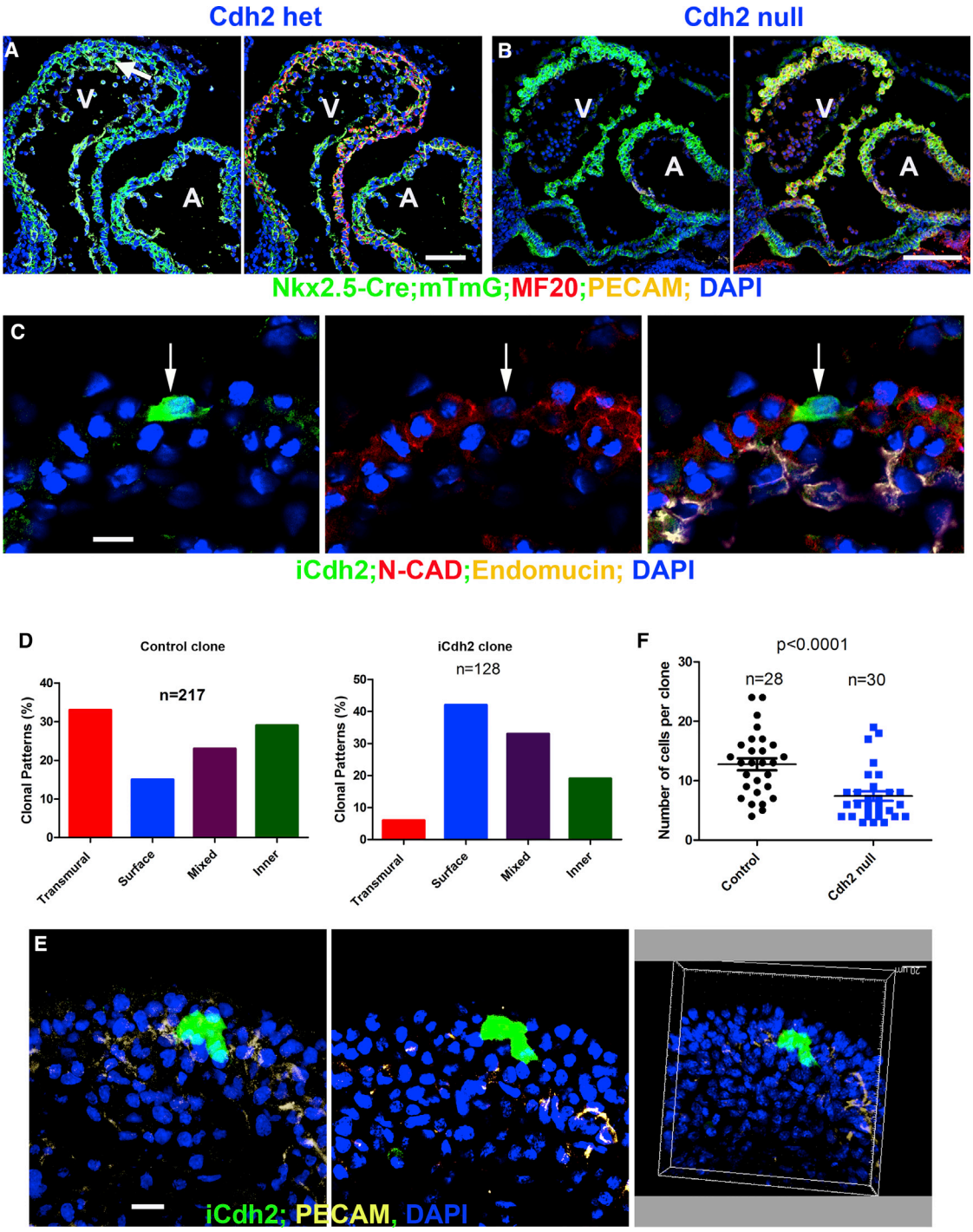


**Figure 5. OCD and Directional Migration Contribute to Trabeculation in an N-CAD-Dependent Manner**

(A and B) Sagittal sections of *Cdh2* heterozygous (A) or *CKO* (B) hearts at E9.5. The arrow points to a trabecula.

(C) N-CAD was not detected in *iCdh2* clone indicated by an arrow.

(D and E) Clonal patterns of control and *iCdh2* (D) and an example of *iCdh2* clone (E). The control is the same as Figure 2H.

(E) Cells in the *iCdh2* were not dispersed. Pictures show two sections from a z stack and a reconstructed 3D picture.

(F) The clonal sizes of *iCdh2* clones are significantly smaller than the control.

Scale bars, 100 μm (A and B) and 10 μm (C and E). A, atrium; V, ventricle.

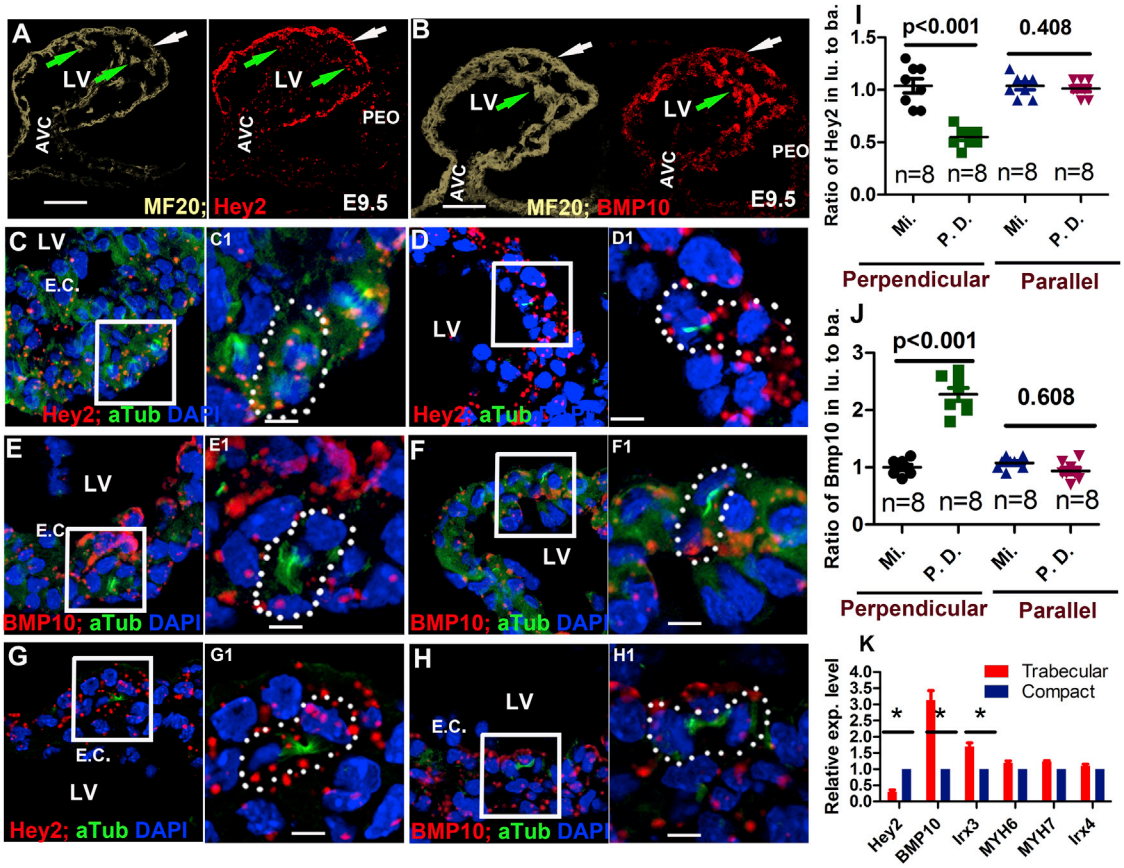


**Figure 6. Extrinsic Asymmetric Cell Division Might Contribute to Asymmetric Expression of Hey2 and BMP10 in Trabecular and Compact Zones**

(A and B) *Hey2* and *BMP10* are asymmetrically distributed to compact and trabecular zones with *Hey2* enriched in the compact zone (A) and *BMP10* enriched in the trabecular zone (B).

(C–H) All show one low-magnification picture to the left and one section of the same cells with higher magnification on the right. (C) *Hey2* and (E) *BMP10* are not asymmetrically distributed in perpendicular dividing cells. After division, when the two daughter cells are separated but still connected at the mid-body, both (D) *Hey2* and (F) *BMP10* are asymmetrically distributed, with the daughter closer to cardiac jelly displaying less *Hey2* and more *BMP10* than the daughter at the heart surface. In parallel division, both *Bmp10* and *Hey2* are symmetrically distributed (G and H) to the two daughter cells.

(I and J) Ratio of *Hey2* (I) and *BMP10* (J) between the two-domains or daughter cells in perpendicular or parallel mitotic or post-division cells (three sections for each cell and n = 8 for each type) is shown.

(K) qPCR data to show the differential expression between trabecular and compact cardiomyocytes harvested by LCM of an E9.5 heart. The experiments were repeated three times.

Scale bars, 100 μm (A and B) and 10 μm (C–H). Lu, luminal; ba, basal; Mi, mitotic; P.D., post-division; E.C., endocardial cells; LV, left ventricle; AVC, atrio-ventricular canal; PEO, pro-epicardial organ.

peptidylprolyl isomerase B and is ubiquitously expressed. We found that mRNA of *Hey2* is strongly expressed in compact cardiomyocytes in the left ventricle of an E9.5 heart, but weakly expressed in trabecular cardiomyocytes (Figure 6A). In contrast, mRNA of *Bmp10* is enriched in trabecular cardiomyocytes of the primitive left ventricle in an E9.5 heart (Figure 6B). As expected, Ppib showed symmetric distribution to compact and trabecular zones (Figure S4A). One potential mechanism contributing to the differential expression of *Hey2* and *Bmp10* in trabecular and compact cardiomyocytes would be the asymmetric distribution of *Hey2* and *Bmp10* in cardiomyocytes that undergo perpendicular OCD. To determine whether perpendicular OCD contributes to regional specification, E9.5 heart sections were stained with acetylated α-tubulin and p120 (an adherens junction-associated protein that marks the membrane) and hybridized with probes to *Bmp10* or *Hey2* mRNA. We counted the number of signal dots or signal intensity in dividing cells and quantified the ratio between the two domains of the dividing cell at telophase or the two daughter cells after the division. We found that the mitotic cells undergoing perpendicular divisions did not display asymmetric distribution of *Hey2* (N = 8) or *Bmp10* (N = 8), as the ratios of *Hey2* or *Bmp10* between the two domains are close to 1 (Figures 6C, 6E, 6I, 6J, and S4B). However, after perpendicular division, when cytokinesis is completed but the two daughter cells are still connected by the midbody, differential *Hey2* and *Bmp10* expression is observed (Figures 6D, 6F, 6I, 6J, S4C, and S4D). In this type of division, the more luminal daughter cell displays more *Bmp10*

and less *Hey2* than the other daughter cell, and the ratio between them for *Hey2* is about 0.5 and for *Bmp10* is about 2 (Figures 6D, 6F, 6I, 6J, S4C, and S4D). In parallel divisions, the asymmetric distribution of Hey2 and BMP10 is not observed (Figures 6G–6I).

As genetic tools to separate trabecular and compact cells are not available, and single-cell analysis from the whole tissue via fluidigm cannot include the geometric location of each cell, we used laser capture microdissection to separate trabecular and compact cardiomyocytes. We captured cardiomyocytes separately from the compact zone and trabecular zone in E9.5 hearts and compared the expression profiles of target genes between the compact and trabecular cells. We found that *Hey2* is highly expressed in compact cells, and *BMP10* and *Irx3* are highly expressed in trabecular cells, whereas expressional levels of *Irx4*, *MYH6*, and *MYH7* are not significantly different (Figure 6K), which is consistent with the ISH results (Figures 6A–6J).

### N-CAD Regulates Trabecular Regional Specification in a Non-Cell-Autonomous Manner

We examined the mRNA expression patterns of *Hey2* and *Bmp10* in *Cdh2 CKO* hearts and found the expression of *Hey2* and *Bmp10* in compact and trabecular cardiomyocytes is different from the controls, with trabecular or inner compact zone expressing similar levels of BMP10 and Hey2 to the compact zone (Figures S5A and S5B; data not shown), indicating a trabecular regional specification defect. The cause of this defect can be non-cell-autonomous, such as through disrupted localization to the cardiac jelly, or cell-autonomous. To distinguish these two possibilities, we induced labeling and deleted *Cdh2* in cells of *iCre;Conf*;*Cdh2*$^{fl/fl}$ hearts by inducing Cre at E7.75 and then tracing for 72 hr. We examined the expression of *Hey2* and *Bmp10* in the *iCdh2* clones. We found that *Bmp10* expression levels in the *iCdh2* clones in the outer compact, inner compact, and trabecular zones are different, with lower *Bmp10* expression in the outer compact zone than in the trabecular zone (Figures S5C and S5D). However, the *Bmp10* levels in *iCdh2* clones of different zones are comparable to those in adjacent control cells (Figures S5C and S5D), indicating that it is the geometric location of the cell and not the N-CAD deletion that determines the differential *Bmp10* expression. Similarly, *Hey2* expression in *iCdh2* clones in the compact zone is higher than in clones in the trabecular zone, and each clone's expression level is not significantly different from that of the surrounding control cells (Figures S5E and S5F). These results indicate that N-CAD regulates the trabecular regional specification non-cell-autonomously by regulating the invasion and migration of cardiomyocytes to different geometric locations where extrinsic signals from cardiac jelly or endocardium may instruct the regional specification.

## DISCUSSION

In mammals, it has been described that trabecular morphogenesis involves the recruitment of cells from the compact zone. However, the cues and the mechanisms underlying cardiomyocyte recruitment are unknown. To address these questions, we investigated trabeculation using single-cell lineage tracing, clonal mosaic models, and tissue-specific knockout mouse models. Our study demonstrates that early stage cardiomyocytes within the forming compact zone undergo OCD and directional migration via an N-CAD-dependent mechanism to contribute to trabeculation. Perpendicular OCD contributes to trabecular morphogenesis and causes daughter cells to be positioned within different geometric locations in the heart and exposed to different extracellular signals, resulting in different specification decisions between the two daughter cells.

### OCD and Directional Migration Contribution to Trabecular Initiation Are N-CAD Dependent

Studies in avian hearts led to the general belief that cardiomyocytes in trabecular and compact myocardium are derived from myocardial progenitor cells that differentiate via local proliferation (Mikawa et al., 1992b; Mikawa and Fischman, 1996). Previous work in zebrafish showed that the myocytes forming the trabeculae arise from a different clonal origin than the cardiomyocytes in the compact zone (Gupta and Poss, 2012; Liu et al., 2010). Conversely, our results demonstrate that trabecular and compact cardiomyocytes within the transmural and mixed clones share the same progenitor cell in the mouse, indicating that at least some compact and trabecular cardiomyocytes arise from a common progenitor cell.

In our single-cell lineage tracing study, the existence of four distinct clonal patterns suggests that the labeled cardiomyocytes might undergo OCD or directional migration during trabeculation. Previous work showed that cardiomyocytes at E13.5 undergo primarily parallel OCD based on IFS (Le Garrec et al., 2013), which is consistent with the heart morphogenesis at E13.5, a stage in which trabecular formation is already completed and the heart undergoes expansion. Hence, a high percentage of parallel OCD would be expected. In this study, we found that 52% of cardiomyocytes at E9.0–E9.5, a stage at which the myocardium initiates trabecular formation, undergo perpendicular OCD, consistent with the observed transmural growth of trabeculae. However, the IFS only allows for observation of cell division patterns at a single window in time, and we would expect that prolonged observation such as time-lapse imaging and lineage tracing of individual cells might be needed to unveil the cellular dynamics during trabeculation. The daughter cells' relative localizations observed in our single-cell lineage tracing for different lengths of time suggest that cardiomyocytes undergo perpendicular OCD during trabeculation (Figure 4C). Perpendicular OCD allows entry of a daughter cell into the cardiac lumen to initiate trabeculation, thereby leading to the formation of the transmural clone (Figures 7A and 7B), which is consistent with previous reports that perpendicular OCD is a polarized cell division and is involved in morphogenesis (Baena-López et al., 2005; Wu et al., 2010). The inner clones indicate that murine cardiomyocytes might undergo cytoskeletal rearrangement (Figures 7A and 7B), become elongated, and migrate toward the heart lumen and contribute to the mass of the trabeculae as previously shown in zebrafish, in which trabeculae are formed by directional migration of cardiomyocytes from the compact zone (Gupta and Poss, 2012; Liu et al., 2010; Peshkovsky et al., 2011; Staudt et al., 2014). The existence of the inner clone is consistent with a recent publication showing that Mesp1 labeled cells form clones inside the mouse heart (Chabab

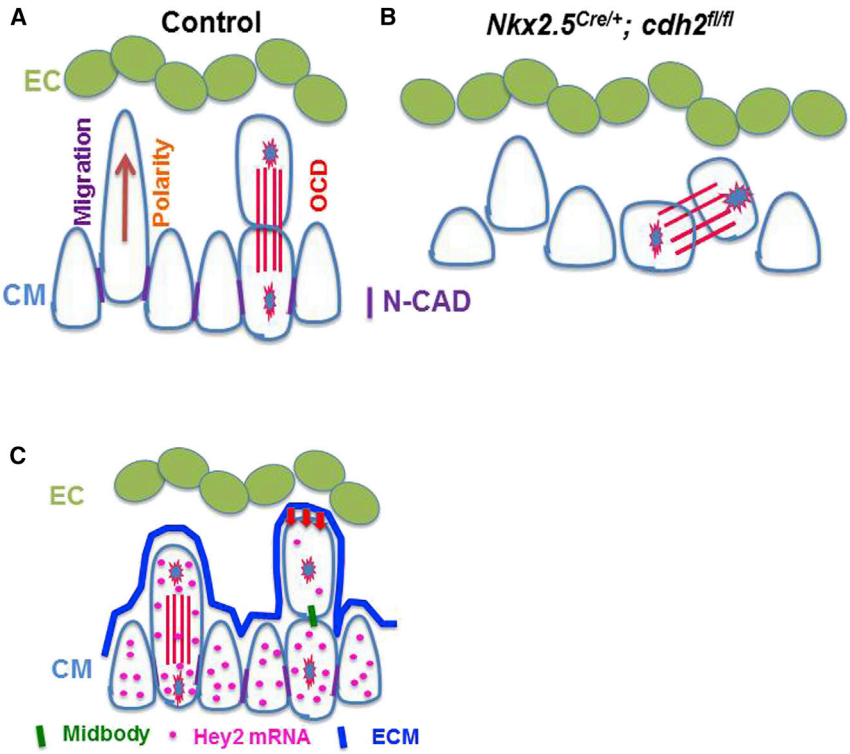


**Figure 7. Models of Trabecular Initiation and Trabecular Regional Specification**

(A and B) OCD and directional migration contribute to trabecular initiation in an N-CAD-dependent manner (A). *Cdh2 null* cells failed to undergo OCD and directional migration (B).

(C) Cardiac jelly and endocardium might provide instructive cues for trabecular regional specification.

et al., 2016). Parallel division of cardiomyocytes results in a surface clone and contributes to the enlargement of the heart (Figures 4A and 4D). However, we cannot exclude the other possibilities of how the clonal patterns are formed and how the trabeculae are initiated, and time-lapse imaging of trabecular morphogenesis in vivo or ex vivo might provide more details.

To study the mechanisms that regulate OCD, *Cdh2* was deleted in whole hearts or single cardiomyocytes. We found that *iCdh2* null clones display abnormal clonal patterns with significantly more surface clones, but fewer transmural clones (Figure 5D), indicating that N-CAD regulates OCD. Furthermore, cells in transmural, mixed, and inner *iCdh2* null clones invade the myocardium less deeply (Figures 3A–3C) and most of the cells of these clones are connected rather than dispersed as in the control (Figures 5E and 2D), indicating that N-CAD is required for cardiomyocyte migration and invasion in addition to establishing OCD (Figures 7A and 7B). Consistently, previous reports showed that adherens junctions were essential to establish mitotic spindle orientation in *Drosophila* (Inaba et al., 2010), in mouse epicardial cells (Wu et al., 2010) and multiple stem cells (Lechler, 2012). That N-CAD is required to establish spindle orientation is demonstrated in in vitro systems such as MDCK cells and MCF10A cells, as disruption of adherens junctions causes the spindle orientation to be random (den Elzen et al., 2009). The lower proliferation rate of the *Cdh2* null cells results in smaller-sized clones, but would not be expected to contribute to clonal pattern changes; instead, the clonal pattern change might be due to the ability of N-CAD to regulate spindle orientation and directional migration.

During trabecular morphogenesis, the appearances of clones that are labeled at different developmental stages are different. Clones labeled at E6.75 displayed dispersive growth, and the clones displayed several cell clusters at E10.5 examined from the heart surface (data not shown), consistent with the fragmentation observed before (Lescroart et al., 2014). However, when the cell labeling is induced at E7.75, fragmentation was not observed, indicating that the timing of labeling affects clonal appearances. Another major factor that contributes to the distinct appearances of the clones is the endocardial cell. Initially, the cells of most clones are dispersed rather being closely associated. At about E9.5, the endocardial cells burrow into myocardium and gradually interact tightly with myocardial cells; this tight interaction forces the cardiomyocytes to integrate and might cause the mixed clone to display a wedge shape at a later stage (Figures S6A and S6B), as previously described (Mikawa et al., 1992a). The differential proliferation rates of cardiomyocytes in different regions can also contribute to the different appearances of the clones (Sedmera et al., 2003).

Other factors in the regulation of cardiomyocyte OCD and migration need to be determined to fully understand this process. Possible candidates are signaling pathways or molecules previously found to be required for trabeculation, such as Brg1/ADAMTS1 (Stankunas et al., 2008), NRG1/ErBb2,4 (Gassmann et al., 1995; Lee et al., 1995; Meyer and Birchmeier, 1995), EphrinB2/EphB4 (Gerety et al., 1999; Wang et al., 1998), BMP10 (Chen et al., 2004), Numb Family Proteins (Wu and Li, 2015; Zhao et al., 2014), Notch signaling (Grego-Bessa et al., 2007), Hand2 (VanDusen et al., 2014), cardiac contraction/hemodynamics (Peshkovsky et al., 2011; Samsa et al., 2015), DAAM1 (Li et al., 2011), and components of the sarcomere and the Z-disk (Finsterer, 2009; Teekakirikul et al., 2013). It will be important to determine whether, and if so how, these players regulate OCD and directional migration.

## Potential Instructive Cues for Trabecular Regional Specification Might Lie in the Cardiac Jelly and Endocardium

Trabecular cardiomyocytes, which take the major responsibility for pumping at early stages of cardiac development, are more

differentiated than compact zone cardiomyocytes (Sedmera et al., 2000). How local proliferation contributes to the distinct differentiation status between compact and trabecular cardiomyocytes remains largely unknown. We discovered that asymmetric expression of *Hey2* and *Bmp10* occurs after, but not before, cytokinesis in perpendicular OCD and that the asymmetric expression is due to the differences in geometric location between the two daughter cells, with the one closer to cardiac jelly displaying more *Bmp10* and less *Hey2* compared to the other daughter cell that is relatively closer to the surface of the heart.

Previous work has shown the intercellular signals between the endocardium and myocardium are essential for trabeculation. These signals include Brg1/ADAMTS1, NRG1/ErBb2,4, EphrinB2/EphB4, Notch, Numb Family Proteins, VEGF, and angiopoietin. At early stages of trabecular initiation, cardiac jelly separates the endocardium from the myocardium and endocardial cells are not physically connected to myocardial cells in most of the regions. However, it could be possible that certain ligands are secreted to the cardiac jelly to facilitate the interaction between endocardium and myocardium (Lai et al., 2010). At later stages, direct Notch ligand and receptor interaction might be involved in the regulation of trabecular cardiomyocyte differentiation, as recent work has shown that overexpression of glycosyltransferase manic fringe in endocardium can causes abnormal expression pattern of Hey2 (D'Amato et al., 2016).

Furthermore, disruption of *Has2*, which is responsible for the synthesis of hyaluronic acid, a major component of cardiac jelly, causes abnormal trabecular morphogenesis (Camenisch et al., 2000; Stankunas et al., 2008), demonstrating the important function of cardiac jelly in trabecular initiation. In addition, *Brg1* in endocardium regulates trabecular morphogenesis by controlling the expression of matrix metalloproteinase ADAMTS1 to modulate cardiac jelly degradation. Our single-cell lineage tracing showed that cells from the same clone that occupy different geometric locations with respect to the cardiac jelly show distinct differentiation status and cells that are adjacent to cardiac jelly display higher *Bmp10* and lower *Hey2* than cells that are close to the heart surface (Figure S7A). The trabecular regional specification defect in *CKO* is not caused by the failure of the *Cdh2* null cells to respond to signaling from the ECM, because the cardiomyocytes in the *Cdh2* null migratory clone display equivalent specification status to the surrounding cells regardless of their proximity to trabecular, compact, or inner zones. Rather, the defect seems to reside in the inability of the *Cdh2* null cells to orient properly in order to migrate toward the cardiac jelly. Based on these data and previous publications (Chen et al., 2013; D'Amato et al., 2016; Grego-Bessa et al., 2007; Lee et al., 1995; Luxán et al., 2013; Meyer and Birchmeier, 1995; Sedmera et al., 2000; VanDusen et al., 2014), it is clear that cues from cardiac jelly and endocardium play an instructive role in cardiomyocyte differentiation (Figure 7C). However, more work will need to be done to reveal the specific cues and signaling pathways that regulate this trabecular specification process. The high relevance of trabeculation defects to human disease warrants future research in the field.

## EXPERIMENTAL PROCEDURES

### Mouse Lines

Mouse lines *Cdh2*$^{fl/fl}$ (Kostetskii et al., 2005), *Rosa26Cre*$^{ERT2}$ (*iCre*) (Badea et al., 2003), *Rosa26-Confetti* (*Conf*) (Livet et al., 2007), and *Rosa26-mTmG* (*mTmG*) (Muzumdar et al., 2007) were purchased from Jackson Laboratory. Dr. Robert Schwartz provided *Nkx2.5*$^{Cre/+}$ mice (Moses et al., 2001). *iCre* males were crossed with *Conf* and *Cdh2*$^{fl/fl}$*;Conf* females to generate, respectively, the following control clones: *iCre;Conf* and *Cdh2* null clones, and *iCre;Conf*;*Cdh2*$^{fl/fl}$ (*iCdh2*) upon tamoxifen induction. All animal experiments are approved by the IACUC at Albany Medical College and were performed according to the NIH Guide for the Care and Use of Laboratory Animals.

### Single mRNA Molecule In Situ Hybridization and Immunofluorescence Staining

In situ hybridization (ISH) and immunofluorescence staining (IFS) were performed according to the protocol of the RNAscope Chromogenic (RED) Assay (cat. no. 310036), which can detect single mRNA molecules. In brief, 24 hr after fixation, the embryos were frozen embedded in OCT compound. Sections of the frozen embedded samples were processed following the step-by-step protocol of the kit. The expressional level of mRNA in each cell was based on the number of mRNA molecules or signal intensity using the confocal scanned pictures, and three scanned sections for each cell were quantified. The numbers of mRNA molecules in cells at comparable locations were also quantified.

### Statistics

Data are shown as mean ± SD. An unpaired, two-tailed Student's t test and chi-square test as specified were used for statistical comparison. A chi-square test was used to compare the division pattern distribution or clonal pattern distribution between control and knockout. A p value of 0.05 or less was considered statistically significant.

Additional materials and methods are available in the Supplementary Information.

## SUPPLEMENTAL INFORMATION

Supplemental Information includes seven figures, one table, and seven movies and can be found with this article online at http://dx.doi.org/10.1016/j.celrep.2016.03.012.

## AUTHOR CONTRIBUTIONS

J.L., L.M., D.S., E.S., and M.W. performed the experiments and analyzed the data. M.W. designed experiments and wrote the paper. A.P. helped the LCM experiments. J.L., G.H., R.J.S., B.Z., A.B.F., and H.A.S. helped the projects.

## ACKNOWLEDGMENTS

We thank M.W. laboratory members for scientific discussion, Dr. Eric N. Olson for insightful comments, Dr. John Schwartz for critical reading, Saiyang Hu and Yangyang Lu for their technical support, and Drs. Joseph Mazurkiewicz and Margarida Barroso for help in imaging. This work is supported by AHA (13SDG16920099) and by National Heart, Lung, and Blood Institute grants (R01HL121700) to M.W. A.P. was supported by an R01 grant HL104251. H.A.S. was supported by an R01 grant HLR01092510.

Received: October 9, 2015
Revised: January 20, 2016
Accepted: February 26, 2016
Published: March 24, 2016

## REFERENCES

Badea, T.C., Wang, Y., and Nathans, J. (2003). A noninvasive genetic/pharmacologic strategy for visualizing cell morphology and clonal relationships in the mouse. J. Neurosci. *23*, 2314–2322.

Baena-López, L.A., Baonza, A., and García-Bellido, A. (2005). The orientation of cell divisions determines the shape of Drosophila organs. Curr. Biol. *15*, 1640–1644.

Breckenridge, R.A., Anderson, R.H., and Elliott, P.M. (2007). Isolated left ventricular non-compaction: the case for abnormal myocardial development. Cardiol. Young *17*, 124–129.

Camenisch, T.D., Spicer, A.P., Brehm-Gibson, T., Biesterfeldt, J., Augustine, M.L., Calabro, A., Jr., Kubalak, S., Klewer, S.E., and McDonald, J.A. (2000). Disruption of hyaluronan synthase-2 abrogates normal cardiac morphogenesis and hyaluronan-mediated transformation of epithelium to mesenchyme. J. Clin. Invest. *106*, 349–360.

Chabab, S., Lescroart, F., Rulands, S., Mathiah, N., Simons, B.D., and Blanpain, C. (2016). Uncovering the Number and Clonal Dynamics of Mesp1 Progenitors during Heart Morphogenesis. Cell Rep. *14*, 1–10.

Chen, H., Shi, S., Acosta, L., Li, W., Lu, J., Bao, S., Chen, Z., Yang, Z., Schneider, M.D., Chien, K.R., et al. (2004). BMP10 is essential for maintaining cardiac growth during murine cardiogenesis. Development *131*, 2219–2231.

Chen, H., Zhang, W., Sun, X., Yoshimoto, M., Chen, Z., Zhu, W., Liu, J., Shen, Y., Yong, W., Li, D., et al. (2013). Fkbp1a controls ventricular myocardium trabeculation and compaction by regulating endocardial Notch1 activity. Development *140*, 1946–1957.

Christoffels, V.M., Keijser, A.G., Houweling, A.C., Clout, D.E., and Moorman, A.F. (2000). Patterning the embryonic heart: identification of five mouse Iroquois homeobox genes in the developing heart. Dev. Biol. *224*, 263–274.

D'Amato, G., Luxán, G., Del Monte-Nieto, G., Martínez-Poveda, B., Torroja, C., Walter, W., Bochter, M.S., Benedito, R., Cole, S., Martinez, F., et al. (2016). Sequential Notch activation regulates ventricular chamber development. Nat. Cell Biol. *18*, 7–20.

den Elzen, N., Buttery, C.V., Maddugoda, M.P., Ren, G., and Yap, A.S. (2009). Cadherin adhesion receptors orient the mitotic spindle during symmetric cell division in mammalian epithelia. Mol. Biol. Cell *20*, 3740–3750.

Devine, W.P., Wythe, J.D., George, M., Koshiba-Takeuchi, K., and Bruneau, B.G. (2014). Early patterning and specification of cardiac progenitors in gastrulating mesoderm. eLife *3*, e03848.

Finsterer, J. (2009). Cardiogenetics, neurogenetics, and pathogenetics of left ventricular hypertrabeculation/noncompaction. Pediatr. Cardiol. *30*, 659–681.

Finsterer, J. (2010). Left ventricular non-compaction and its cardiac and neurologic implications. Heart Fail. Rev. *15*, 589–603.

Gassmann, M., Casagranda, F., Orioli, D., Simon, H., Lai, C., Klein, R., and Lemke, G. (1995). Aberrant neural and cardiac development in mice lacking the ErbB4 neuregulin receptor. Nature *378*, 390–394.

Gerety, S.S., Wang, H.U., Chen, Z.F., and Anderson, D.J. (1999). Symmetrical mutant phenotypes of the receptor EphB4 and its specific transmembrane ligand ephrin-B2 in cardiovascular development. Mol. Cell *4*, 403–414.

Grego-Bessa, J., Luna-Zurita, L., del Monte, G., Bolós, V., Melgar, P., Arandilla, A., Garratt, A.N., Zang, H., Mukouyama, Y.S., Chen, H., et al. (2007). Notch signaling is essential for ventricular chamber development. Dev. Cell *12*, 415–429.

Gupta, V., and Poss, K.D. (2012). Clonally dominant cardiomyocytes direct heart morphogenesis. Nature *484*, 479–484.

Hama, H., Kurokawa, H., Kawano, H., Ando, R., Shimogori, T., Noda, H., Fukami, K., Sakaue-Sawano, A., and Miyawaki, A. (2011). Scale: a chemical approach for fluorescence imaging and reconstruction of transparent mouse brain. Nat. Neurosci. *14*, 1481–1488.

Inaba, M., Yuan, H., Salzmann, V., Fuller, M.T., and Yamashita, Y.M. (2010). E-cadherin is required for centrosome and spindle orientation in Drosophila male germline stem cells. PLoS ONE *5*, e12473.

Jenni, R., Rojas, J., and Oechslin, E. (1999). Isolated noncompaction of the myocardium. N. Engl. J. Med. *340*, 966–967.

Knoblich, J.A. (2008). Mechanisms of asymmetric stem cell division. Cell *132*, 583–597.

Kochilas, L.K., Li, J., Jin, F., Buck, C.A., and Epstein, J.A. (1999). p57Kip2 expression is enhanced during mid-cardiac murine development and is restricted to trabecular myocardium. Pediatr. Res. *45*, 635–642.

Koibuchi, N., and Chin, M.T. (2007). CHF1/Hey2 plays a pivotal role in left ventricular maturation through suppression of ectopic atrial gene expression. Circ. Res. *100*, 850–855.

Kostetskii, I., Li, J., Xiong, Y., Zhou, R., Ferrari, V.A., Patel, V.V., Molkentin, J.D., and Radice, G.L. (2005). Induced deletion of the N-cadherin gene in the heart leads to dissolution of the intercalated disc structure. Circ. Res. *96*, 346–354.

Lai, D., Liu, X., Forrai, A., Wolstein, O., Michalicek, J., Ahmed, I., Garratt, A.N., Birchmeier, C., Zhou, M., Hartley, L., et al. (2010). Neuregulin 1 sustains the gene regulatory network in both trabecular and nontrabecular myocardium. Circ. Res. *107*, 715–727.

Le Garrec, J.F., Ragni, C.V., Pop, S., Dufour, A., Olivo-Marin, J.C., Buckingham, M.E., and Meilhac, S.M. (2013). Quantitative analysis of polarity in 3D reveals local cell coordination in the embryonic mouse heart. Development *140*, 395–404.

Lechler, T. (2012). Adherens junctions and stem cells. Subcell. Biochem. *60*, 359–377.

Lee, K.F., Simon, H., Chen, H., Bates, B., Hung, M.C., and Hauser, C. (1995). Requirement for neuregulin receptor erbB2 in neural and cardiac development. Nature *378*, 394–398.

Lescroart, F., Chabab, S., Lin, X., Rulands, S., Paulissen, C., Rodolosse, A., Auer, H., Achouri, Y., Dubois, C., Bondue, A., et al. (2014). Early lineage restriction in temporally distinct populations of Mesp1 progenitors during mammalian heart development. Nat. Cell Biol. *16*, 829–840.

Li, D., Hallett, M.A., Zhu, W., Rubart, M., Liu, Y., Yang, Z., Chen, H., Haneline, L.S., Chan, R.J., Schwartz, R.J., et al. (2011). Dishevelled-associated activator of morphogenesis 1 (Daam1) is required for heart morphogenesis. Development *138*, 303–315.

Liu, J., Bressan, M., Hassel, D., Huisken, J., Staudt, D., Kikuchi, K., Poss, K.D., Mikawa, T., and Stainier, D.Y. (2010). A dual role for ErbB2 signaling in cardiac trabeculation. Development *137*, 3867–3875.

Livet, J., Weissman, T.A., Kang, H., Draft, R.W., Lu, J., Bennis, R.A., Sanes, J.R., and Lichtman, J.W. (2007). Transgenic strategies for combinatorial expression of fluorescent proteins in the nervous system. Nature *450*, 56–62.

Luo, Y., Ferreira-Cornwell, M., Baldwin, H., Kostetskii, I., Lenox, J., Lieberman, M., and Radice, G. (2001). Rescuing the N-cadherin knockout by cardiac-specific expression of N- or E-cadherin. Development *128*, 459–469.

Luxán, G., Casanova, J.C., Martínez-Poveda, B., Prados, B., D'Amato, G., MacGrogan, D., Gonzalez-Rajal, A., Dobarro, D., Torroja, C., Martinez, F., et al. (2013). Mutations in the NOTCH pathway regulator MIB1 cause left ventricular noncompaction cardiomyopathy. Nat. Med. *19*, 193–201.

Meilhac, S.M., Kelly, R.G., Rocancourt, D., Eloy-Trinquet, S., Nicolas, J.F., and Buckingham, M.E. (2003). A retrospective clonal analysis of the myocardium reveals two phases of clonal growth in the developing mouse heart. Development *130*, 3877–3889.

Meilhac, S.M., Esner, M., Kerszberg, M., Moss, J.E., and Buckingham, M.E. (2004). Oriented clonal cell growth in the developing mouse myocardium underlies cardiac morphogenesis. J. Cell Biol. *164*, 97–109.

Meyer, D., and Birchmeier, C. (1995). Multiple essential functions of neuregulin in development. Nature *378*, 386–390.

Mikawa, T., and Fischman, D.A. (1996). The polyclonal origin of myocyte lineages. Annu. Rev. Physiol. *58*, 509–521.

Mikawa, T., Borisov, A., Brown, A.M., and Fischman, D.A. (1992a). Clonal analysis of cardiac morphogenesis in the chicken embryo using a replication-defective retrovirus: I. Formation of the ventricular myocardium. Dev. Dyn. *193*, 11–23.

Mikawa, T., Cohen-Gould, L., and Fischman, D.A. (1992b). Clonal analysis of cardiac morphogenesis in the chicken embryo using a replication-defective retrovirus. III: Polyclonal origin of adjacent ventricular myocytes. Dev. Dyn. *195*, 133–141.

Moses, K.A., DeMayo, F., Braun, R.M., Reecy, J.L., and Schwartz, R.J. (2001). Embryonic expression of an Nkx2-5/Cre gene using ROSA26 reporter mice. Genesis *31*, 176–180.

Muzumdar, M.D., Tasic, B., Miyamichi, K., Li, L., and Luo, L. (2007). A global double-fluorescent Cre reporter mouse. Genesis *45*, 593–605.

Ong, L.L., Kim, N., Mima, T., Cohen-Gould, L., and Mikawa, T. (1998). Trabecular myocytes of the embryonic heart require N-cadherin for migratory unit identity. Dev. Biol. *193*, 1–9.

Peshkovsky, C., Totong, R., and Yelon, D. (2011). Dependence of cardiac trabeculation on neuregulin signaling and blood flow in zebrafish. Dev. Dyn. *240*, 446–456.

Pignatelli, R.H., McMahon, C.J., Dreyer, W.J., Denfield, S.W., Price, J., Belmont, J.W., Craigen, W.J., Wu, J., El Said, H., Bezold, L.I., et al. (2003). Clinical characterization of left ventricular noncompaction in children: a relatively common form of cardiomyopathy. Circulation *108*, 2672–2678.

Samsa, L.A., Givens, C., Tzima, E., Stainier, D.Y., Qian, L., and Liu, J. (2015). Cardiac contraction activates endocardial Notch signaling to modulate chamber maturation in zebrafish. Development *142*, 4080–4091.

Sedmera, D., and Thomas, P.S. (1996). Trabeculation in the embryonic heart. BioEssays *18*, 607.

Sedmera, D., Pexieder, T., Vuillemin, M., Thompson, R.P., and Anderson, R.H. (2000). Developmental patterning of the myocardium. Anat. Rec. *258*, 319–337.

Sedmera, D., Reckova, M., DeAlmeida, A., Coppen, S.R., Kubalak, S.W., Gourdie, R.G., and Thompson, R.P. (2003). Spatiotemporal pattern of commitment to slowed proliferation in the embryonic mouse heart indicates progressive differentiation of the cardiac conduction system. Anat. Rec. A Discov. Mol. Cell. Evol. Biol. *274*, 773–777.

Stankunas, K., Hang, C.T., Tsun, Z.Y., Chen, H., Lee, N.V., Wu, J.I., Shang, C., Bayle, J.H., Shou, W., Iruela-Arispe, M.L., and Chang, C.P. (2008). Endocardial Brg1 represses ADAMTS1 to maintain the microenvironment for myocardial morphogenesis. Dev. Cell *14*, 298–311.

Staudt, D.W., Liu, J., Thorn, K.S., Stuurman, N., Liebling, M., and Stainier, D.Y. (2014). High-resolution imaging of cardiomyocyte behavior reveals two distinct steps in ventricular trabeculation. Development *141*, 585–593.

Susaki, E.A., Tainaka, K., Perrin, D., Kishino, F., Tawara, T., Watanabe, T.M., Yokoyama, C., Onoe, H., Eguchi, M., Yamaguchi, S., et al. (2014). Whole-brain imaging with single-cell resolution using chemical cocktails and computational analysis. Cell *157*, 726–739.

Teekakirikul, P., Kelly, M.A., Rehm, H.L., Lakdawala, N.K., and Funke, B.H. (2013). Inherited cardiomyopathies: molecular genetics and clinical genetic testing in the postgenomic era. J. Mol. Diagn. *15*, 158–170.

Towbin, J.A., Lorts, A., and Jefferies, J.L. (2015). Left ventricular non-compaction cardiomyopathy. Lancet *386*, 813–825.

VanDusen, N.J., Casanovas, J., Vincentz, J.W., Firulli, B.A., Osterwalder, M., Lopez-Rios, J., Zeller, R., Zhou, B., Grego-Bessa, J., De La Pompa, J.L., et al. (2014). Hand2 is an essential regulator for two Notch-dependent functions within the embryonic endocardium. Cell Rep. *9*, 2071–2083.

Wang, H.U., Chen, Z.F., and Anderson, D.J. (1998). Molecular distinction and angiogenic interaction between embryonic arteries and veins revealed by ephrin-B2 and its receptor Eph-B4. Cell *93*, 741–753.

Weiford, B.C., Subbarao, V.D., and Mulhern, K.M. (2004). Noncompaction of the ventricular myocardium. Circulation *109*, 2965–2971.

Wu, M., and Li, J. (2015). Numb family proteins: novel players in cardiac morphogenesis and cardiac progenitor cell differentiation. Biomol. Concepts *6*, 137–148.

Wu, M., Smith, C.L., Hall, J.A., Lee, I., Luby-Phelps, K., and Tallquist, M.D. (2010). Epicardial spindle orientation controls cell entry into the myocardium. Dev. Cell *19*, 114–125.

Zhang, W., Chen, H., Qu, X., Chang, C.P., and Shou, W. (2013). Molecular mechanism of ventricular trabeculation/compaction and the pathogenesis of the left ventricular noncompaction cardiomyopathy (LVNC). Am. J. Med. Genet. C. Semin. Med. Genet. *163C*, 144–156.

Zhao, C., Guo, H., Li, J., Myint, T., Pittman, W., Yang, L., Zhong, W., Schwartz, R.J., Schwarz, J.J., Singer, H.A., et al. (2014). Numb family proteins are essential for cardiac morphogenesis and progenitor differentiation. Development *141*, 281–295.